

SRI DATA ON CHINESE  
PHOTODIODE EXPERIMENTS

SG1E

Approved For Release 2000/08/11 : CIA-RDP96-00792R000300280001-4

Approved For Release 2000/08/11 : CIA-RDP96-00792R000300280001-4

TAB

ABstract

# 云 大 学

The strange phenomena of paranormal functions of the human body affecting on a photosensitive Diode

by Zheng Tian Min, Zhe Nian Lin, Luo Xin, Mu Jun, Chen Guo Chai  
(Yunnan University) Li Hong Yi (Wuhan University)

## Abstract

The strange phenomena produced on a photosensitive diode held in the palm of a child with paranormal function are report in this paper. The Characteristic-Curve Tracer indicates that by concentrating their mind upon their palms, or "working", the children with paranormal function can emit unknown radiation, which can induce abnormal change in the photosensitive diode and alter the characteristic curve thereof. The chief features of such changes are as follows:

1. A negative emf is produced even when the photosensitive diode is covered with a piece of black paper.
2. The back resistance is conspicuously reduced and the leakage current increased surprisingly.
3. The closed loop of the reverse characteristic curve which is due to the defects of the diode is subject to phase changes during the "working".
4. There is no apparent difference in the above mentioned phenomena during the course of the experiment whether a piece of black paper is placed between the diode and the palm or not.
5. The characteristic curve is restored to its normal state when the child stops his or her "working".

After magnifying the paranormal change with a radiometer amplifier, the output potential variations are displayed with an X-Y record. It is found that the unknown radiation is closely related to the paranormal function. The following important features are observed.

1. The children with paranormal function produce negative readings on the radiometer in comparison with the positive readings obtained when light radiation is received.
2. There are differences of 2-3 order of magnitude in the potential changes produced between normal children and those gifted with paranormal functions. The latter are  $10^{-10}$ , whereas the former are  $10^{-12}$ .
3. The results obtained when the gifted children are "working" and when they are not "working" with the diode are conspicuously different. The values are zero when they are not "working".
4. When the gifted children were in the course of recognizing hidden letters, or practising telepathy or PK, the curves on the X-Y recorder are closely related to those displayed in the course of "working" with the diode, rising from the beginning of "working" and dropping to the zero level at the end of "working".
5. When the gifted children were watching the recording apparatus, the resulting readings were higher. It seems that there appeared an action of conscious feedback.

# 云 南 大 学

o. There are great differences in the graphic recordings for different individuals among the gifted children.

7. In comparing measurement on the X-Y recorder for mind concentration upon the palms between practitioners of Chinese martial arts and the gifted children, the children showed higher measurements on the average, although a few martial arts practitioners also scored high.

The above results indicate that the photosensitive device is a suitable device for measuring objectively the strange information emitted by children with paranormal functions.

published in "Nature Journal" 4.8.(1981)

TAB

Original Paper

# 人体特异功能在一种光敏探头上的异常现象

郑天民 朱念麟 罗新木 钱 陈国才 (云南大学)  
李洪仪 (武汉大学)

一年来,我国人体特异功能的研究已经由信息传递与接收、处理,发展到特异功能致动的水平。对这些特异现象的物理和生理等各方面的观察和实验正在广泛地设计和进行。我们认为,所有这些特异现象的出现都和“特异功能”儿童所发未知辐射与物质的相互作用有关。最近,我们进行了一组特异辐射与物质相互作用的实验。并利用这一结果,通过辐射仪对具特异功能儿童的“发功”过程进行了图象描述记录,得到了一些有意义的结果。现将实验结果整理报告如下。

我们用辐射仪对具特异功能的儿童小孙、小邵、小杨、小陈等,在用特异功能认字、辨色、拨钟表和致动等特异功能状态下的“发功”过程进行测量。(在作上述特异功能的同时,将辐射仪探头置于手心或腋下,从而进行测量。)在这个过程中,发现辐射仪的数码显示出现负读数(辐射仪在室温、无辐射时调零)。为了找寻负读数出现的原因,我们发现:特异功能儿童发功时,改变了该仪器探头的物理特性这一特异现象。

辐射仪的探头是灵敏度为  $10^{-7} \text{W/cm}^2$ , 测量有效响应在  $190 \sim 1100 \text{nm}$  范围内的光敏二极管。在遮光条件下(如图 1),用 JT-1 型图示仪测量其晶体管反向特性曲线时,当 Y 轴取集电极电流  $0.01 \text{毫安}/\text{度档}$ , X 轴取集电极电压为  $0.5 \text{伏}/\text{度档}$ , 峰值电压调至  $-6 \text{伏}$  左右,限流电阻取  $1 \text{k}\Omega$  时,图示仪荧光屏上出现如图 2(a) 所示之正常二极管反向特性曲线。在实验测

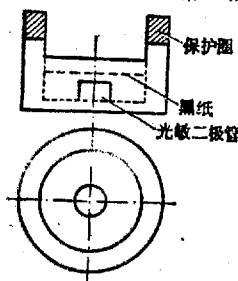


图 1

量之前,我们用黑纸遮光,在探头前加上高为 1 厘米的保护圈(如图 1),以防止受试者手心直接接触二极管,然后将探头交给受试者,握在手中,手心(劳宫穴)对着探头窗口。当她们“发功”(即处于特异功能状态)时,曲线立即

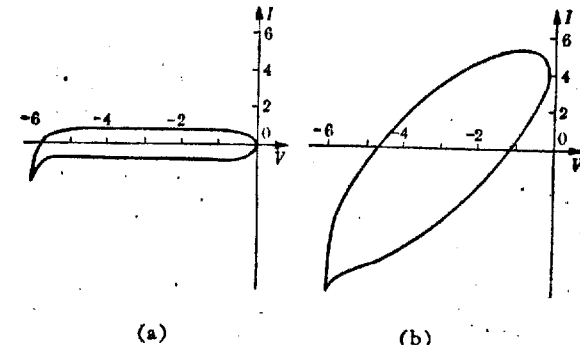


图 2 (a) 正常状态下二极管反向特性曲线 (b) 特异功能作用下上述二极管反向特性曲线

改变形状,呈现出如图 2(b) 所示之曲线。

由图 2(b) 可得一些重要结果:

1. 由图示仪刻度读数发现,在原零点电位处,曲线右端升高,上升的大小与特异功能的强弱有关,最大可达五格左右。相当于产生了约 50 毫伏的电动势。

2. 同时,曲线向左下方倾斜,显示漏电流增大,相当于并联了一个几十  $k\Omega$  的线性电阻(如图 3)。

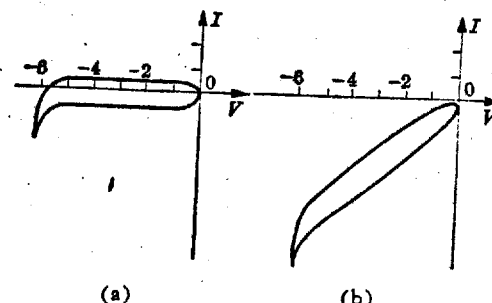


图 3 (a) 探头二极管反向特性 (b) 并联一个  $50k\Omega$  电阻时探头二极管的反向特性

3. 把图 2(b) 与图 3(b) 相比较,除了曲线在 Y 轴升高以外,还出现闭合曲线变肥的现象,这可能是由于正常信号与发功信号之间产生了一个位相差所造成

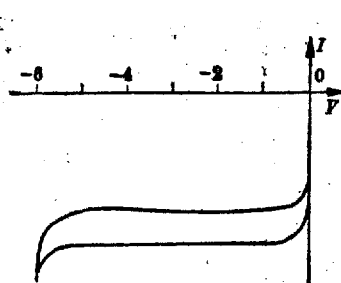


图 4 光照时探头二极管的反向特性

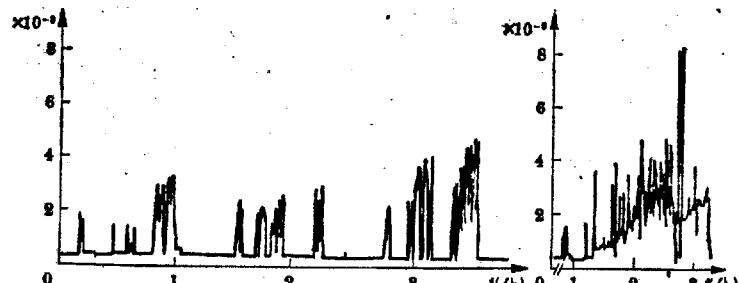


图 5 (a) (b)

的结果，在发功过程中，曲线有“胖”、“瘦”的变化，说明位相差在发功过程中也相应变化。

4. 为排除可见光的干扰，在探头上加黑纸遮掩。测量结果与不加黑纸的结果相同，这说明加了黑纸对特异辐射似乎没有影响。

为了考查温度的影响，我们将探头放在冰块上，仪器显示为零，而不显示负读数。

5. 当“发功”停止时，二极管立即恢复原来的特性曲线。

光敏二极管探头接收光信号时所产生的常规特性曲线，如图 4 所示，光电流表现为整个曲线向下平移。显然，它与图 2 (b)是大不相同的。

由以上几点说明，光敏二极管探头可能接收到一种不同于该管所响应的接收范围内的未知辐射，它与探头相互作用使其特性曲线发生了变化，而形成这种特异现象。同时，也说明这种光敏二极管可能对“特异辐射”敏感。

## 二

尽管我们利用辐射仪不一定 是 测量到常规的 190~1100nm (近紫外到近红外) 波段的电磁波辐射。但是，测量结果表明，仪器所显示的负读数的变化规律，与特异功能儿童的发功状态密切相关。在某种意义上，可以说，捕捉到了记录特异功能儿童发功的某

种客观信息指标。它表现出发功的某种明显的规律性，并且对照了特异功能儿童与一般人集中意识产生的差别；同时还显示特异功能儿童发功与某种类型的气功师一致，而与另一类气功师不同等一些有价值的结果。

1. 特异功能儿童与一般人的被测信号有显著差别：

在多次测量过程中，我们发现具特异功能的儿童和某些气功师在发功时，测得其负读数可达  $10^{-8} \sim 10^{-7}$  ( $W/cm^2$ ) 的数量级 (图 5 a)。然而一般人和另一类气功师，尽管意识高度集中于探头，但是仍然不能出现负读数。有的人虽然也能产生负读数，但其数量级至多也只能达到  $10^{-6} \sim 10^{-5}$  ( $W/cm^2$ ) (图 5 b)。两相比较，读数相差二至三个数量级。

2. 特异功能儿童发功与不发功有明显差别：

(1) 正如我们在《人体特异功能力学效应的初步测试》一文<sup>[1]</sup>中描述的现象一样，图示仪再次记录到与特异功能相关的一个个脉冲。

(2) 在对特异功能儿童测量过程中，意识状态占有极重要的地位。当她们集中意识时，负读数骤然增大；而当她们精力分散、谈话时，负读数立即下降；不发功时，读数很快回到零指示。一般人虽然有时也有负读数出现，但是，读数不仅只是在  $10^{-6} \sim 10^{-5}$  左右，而且还没有明显的意识调制效应。图 6 的曲线是在不同的意识状态下，特异功能儿童小孙的测量结果。

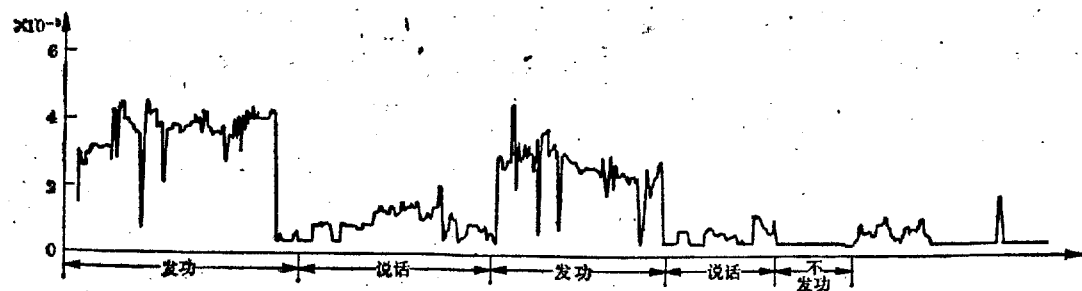


图 6

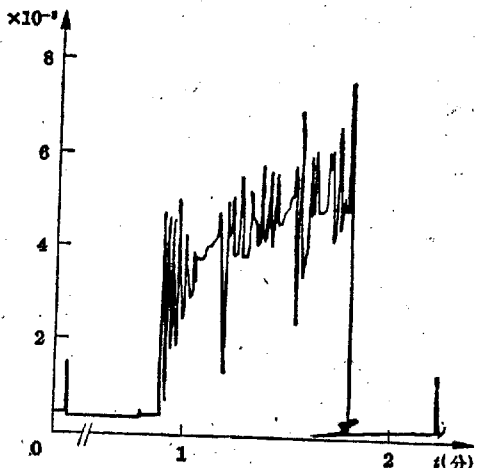


图 7

3. 特异功能儿童作功(认字、思维传感、拨钟表、致动等)时,被测信号与发功过程有明显的、有规律的相关性:

为了研究特异功能儿童在接收信息和致动时与我们所记录到的信息之间的相关性,我们让特异功能儿童在认字、思维传感认字、拨钟和“致动”的同时,描述其特异辐射,得到图7至图11的一组曲线。这些曲线表明,特异功能儿童作功时,与所记录到的信息是密切相关的。在作功时,特异功能儿童普遍存在一个能量存储、集积的过程,它在曲线上表现为脉冲式地不断的上升。经过这段必要的“准备”时间后,作功便取得结果。一旦取得结果,特异功能儿童便不再发功,曲线回到零点。

图7是小孙认字,用了不到一分钟的时间认出,在此过程中,曲线在脉冲式地不断上升,认出字时,数字显示最高,读数为 $7 \times 10^{-3}$ 。

图8是小邵和小孙传感认字,小邵手拿探头,小

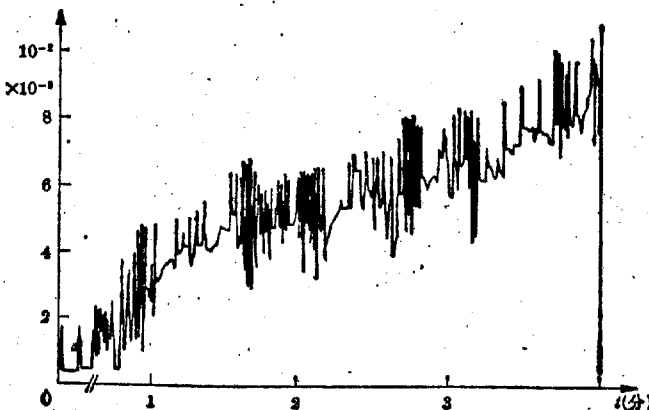


图 8

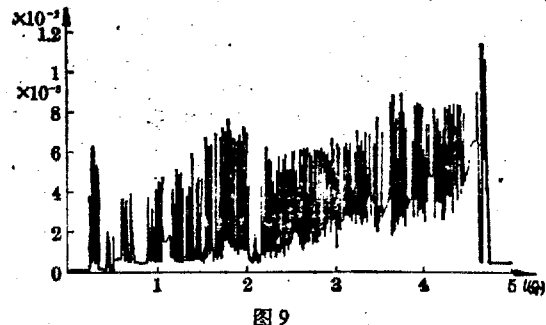


图 9

孙手握字条,经三分半钟,二人同时准确认出,此时辐射仪数字显示最高,达到 $1 \times 10^{-2}$ 。

图9是小孙“拨钟”实验,她一手握探头,一手摸小座钟(座钟已改装,外部无可动部分,说明见[1]),经四分半钟,以特异功能把钟拨动,此时数字显示最高,读数为 $1.15 \times 10^{-2}$ 。

图10是小孙用“特异功能取物”的实验记录,她用了两分多钟,取来一朵小花,最高数字显示为 $1.56 \times 10^{-2}$ 。在接近完成时,功能的脉冲起伏十分巨大。

在测量中,绝大多数认字的结果都是正确的,但有时也有认错的情况,如图11所示,小邵经2分23秒报告说认出字了,但核对结果是错误的。然而,在认字过程中,仍然接收到辐射变化的信息,与正确认字的结果并无二致。

由图7至图11的曲线峰值比较可看出,曲线的最大峰值与作功的难度基本对应,如认字时只是 $7 \times$

$10^{-3}$ ,取花时达到 $1.56 \times 10^{-2}$ 以上。

#### 4. 意识反馈作用:

图12所示曲线是特异功能儿童在作功时,注视数字显示器所形成的。图11所得的曲线值高一倍到十倍,说明儿童在作实验过程中,通过意识反馈,来加强这种反馈效应,数码显示最大值和变化是很有意义的,是十分重要的。从这种反馈作用对研究特异功能儿童来说,所以会截然不同的原因。

#### 5. 特异功能儿童之差异:

图9是小孙拨钟,显示了清晰的脉冲;图5a和图13

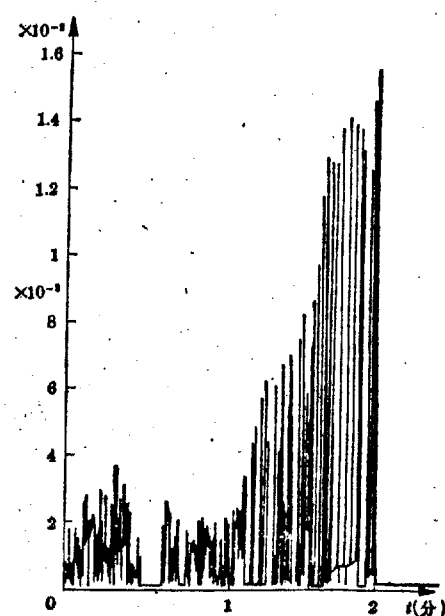
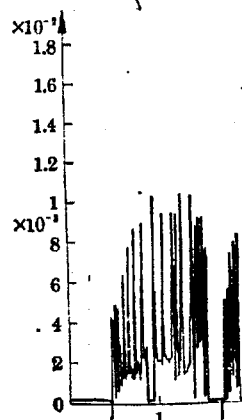


图 10



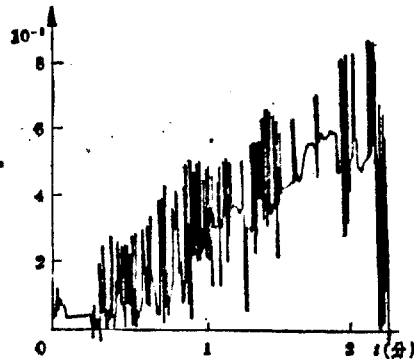


图11

同时准确认出，此时  
 $10^{-3}$ 。  
 ②一手握探头，一手摸  
 动部分，说明见[1])，  
 摆动，此时数字显示最

物”的实验记录，她用  
 变高数字显示为 $1.56 \times 10^{-3}$ 。  
 脉冲起伏十分巨大。  
 的结果都是正确的，但  
 小邵经2分23秒  
 是错误的。然而，在认  
 识的信息，与正确认字  
 比较可看出，曲线的最  
 如认字时只是 $7 \times$

$10^{-3}$ ，取花时达到 $1.56 \times 10^{-3}$ ，功能强度增长了一倍以上。

#### 4. 意识反馈作用：

图12所示曲线是特异功能儿童在测量过程中眼睛注视数字显示器所形成的较高值曲线，它比图7至图11所得的曲线值高一倍到几倍。这是由于具特异功能儿童在作实验过程中，眼睛接收了显示信号，然后通过意识反馈，来加强这种特异辐射，形成辐射的正反馈效应，数码显示最大值达 $1.8 \times 10^{-3}$ 的数量级。这种反馈作用对研究特异功能儿童各生理状态的相互联系和变化是很有意义的，同时对研究儿童心理状态也是十分重要的。从这种反馈作用，就可以解释特异功能儿童在心情愉快和气恼不悦这两种状态下作功的效果所以会截然不同的原因。

5. 特异功能儿童之间所记录下的信息彼此差别甚大：

图9是小孙拔钟，显示时间约1秒的一个个很密集的脉冲，图5a和图13是小杨和小陈的特功曲线，表

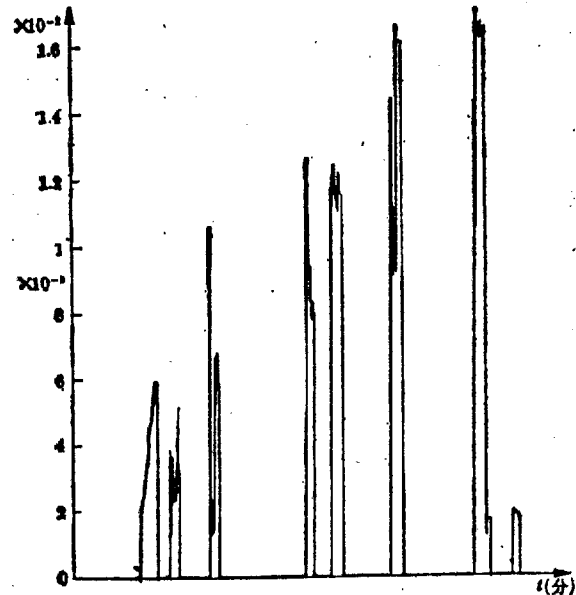


图13

现为时间间隔相当宽的一个个分离的脉冲，脉冲宽度约0.2秒，上升前沿小于 $10^{-3}$ 秒，而幅度较大，约比小孙、小邵大一个数量级。这与她们在特异功能实验时的情况有密切的相关性，小孙的特异功能是相对比较稳定的。

#### 6. 气功师的测量信息彼此差别甚大：

我们邀请了一些气功师来做实验，记录到属于外功型(或发射型)的气功师，基本上得不到负值读数。如唐瑞林同志作了多次实验都得到大于零的结果，而内功型(或接收型)的气功师又有两种情况：一是测量记录与一般人同一数量级，仅只在 $10^{-6}$ 数量级上显示出负值的结果(如图14)，然而从曲线可以看到气功师孙全意识控制的稳定上升，与特异功能儿童发功时显示的脉冲大不相同，与一般人的波动也不相同。二是内功敏感型气功师，发功时，可以得到与特异功能儿童类似的结果，数量级也相同，如某研究所范剑峰同志。因此，虽然气功与特异功能都可能是一种大脑意识活动高度集中后出现的人体特异状态，但是我们所测量到的这类信息中，不仅它们彼此有区别，而且特异功能儿童之间也各各有别，各类气功师之间也有明显差别。这对我们进一步研究人体科学是具有重要意义的。

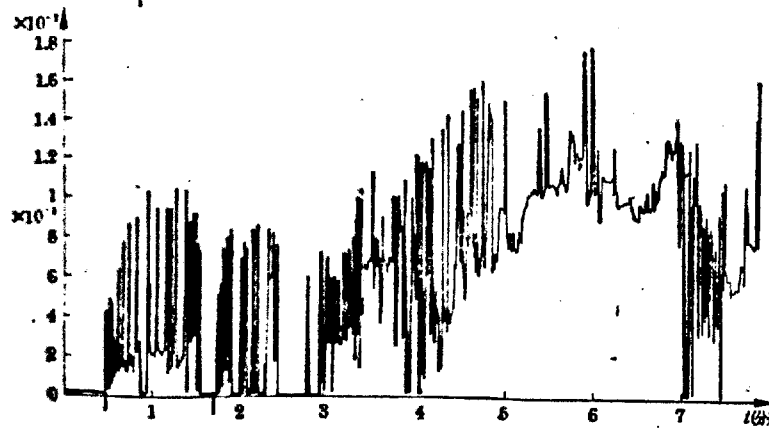


图12

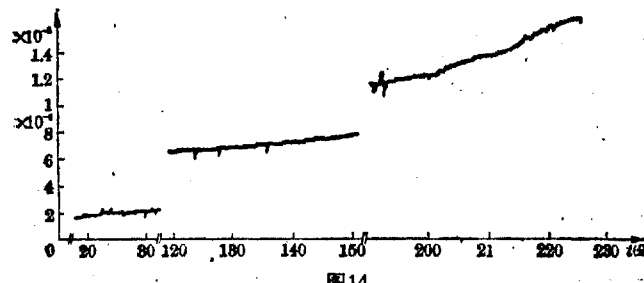


图14

## 三

1. 通过以上讨论, 我们得出特异功能与辐射仪探头内二极管的物质所发生的相互作用形式是与常规测量时截然不同的另一种信息载体物质, 我们暂称为“特异辐射”。通过一系列的实验, 我们发现它与特异功能儿童作功的各类特异现象密切相关。因此对这一现象的深入研究有助于探讨特异功能的物理学机制、生理学机制等一系列本质问题。

2. 这个实验使我们对特异功能的某些现象的解释, 提供了有利的线索。例如, 特异功能儿童“拨动”电子表、以及使发射机信息变弱和中断等现象, 由于晶体管特性曲线在特异功能影响下会发生变化, 这就为解释这些现象提供了一种可能性。

3. 我们在用 2CU 系列、2AP 系列等一些常见二极管进行测试时, 有的毫无反应, 有的虽然有反应, 但是重复率极低, 并且没有出现“特异电动势”, 仅有漏电流增大的现象产生。这说明特异辐射的探测需选用适当的器件, 因此特异辐射的探测与器件的结构类

型、材料等有关, 同时与器件灵敏度关系也很大。

4. 由于这一特异相互作用现象的发现, 使我们对过去所进行的一些人体特异状态的物理量的测量提出了新的置疑。正如我们通过辐射仪测量到的, 并不一定是负辐射, 也不一定是频率在 190~1100nm 范围内的电磁辐射一样, 过去所测到的红外、静电、磁等效应和测量数值, 到底是探头本身在特异辐射作用下发生的非常规变化导致的相对误测量结果, 还是真实、正确的客观测量结果? 值得重新研究和校正, 因为在人体科学中, 未知因素仍然很多。

5. 尽管我们捕捉到了特异功能的某种信息, 但是目前尚不知道这种信息及其载体的本质所在, 不能断言这种信息是特异功能的本质信息, 尤其对特异功能致动而言更是如此。因为能量如此微弱的信息, 是难于对非生物体完成特异功能致动的宏观效应的。因此, 从特异功能的各种现象来看, 这种“特异辐射”可能只是一种伴生信息或二次效应。所以尚需进一步找寻特异功能致动的宏观效应载体。

在我们进行实验过程中, 和云南大学无线电系副主任郑苏民副教授进行了有意义的讨论。云南大学物理系副主任刘佩文、讲师张世鸾、陈星奎和王永熙等同志参加了部分观察和讨论, 杨毓林、张正华提供了部分设备, 特此表示衷心感谢。

[1] 云南大学人体特异功能研究组, 《自然杂志》, 4 (1981) 348

TAB

SRI Analysis

THE STRANGE PHENOMENON OF PARANORMAL FUNCTIONS OF THE HUMAN BODY  
EFFECTING ON A PHOTOSENSITIVE DIODE:  
ANALYSIS AND RECOMMENDATIONS FOR FURTHER STUDY

Experimental Procedure

SG1A

Based upon the abstract provided, original figure captions and [REDACTED] the following experimental procedures and apparatus appear to have been utilized for the first set of experiments:

- A photodiode with a sensitivity of  $10^{-7}$  watts  $\text{cm}^{-2}$  in a bandwidth of 190-1100 nm was used. From Sze\* (Figure 24 on attachments) we expect this to be a silicon device.
- The photodiode was contained in a "well" of some sort surrounded by a "protection ring" and covered with black paper. At present the thermal and electrical properties of this encapsulation are unknown.
- A characteristic curve tracer (Model JT-1) was used to reverse bias the diode and measure its voltage-current response under various conditions.
- The curve tracer was set up so that the voltage axis was .5 V per dimension and the current .01 mA/div. Diode breakdown (the "knee" of the curve) was -6V with a 1 K $\Omega$  current limiting resistor.

Each subject then held the photodiode assembly in their palm and attempted to influence the device. Successful experiments were marked by change in the I/V characteristic from that typical of a diode to one more like a resistor with some parallel capacitance as seen in Figure 2b.<sup>†</sup> In fabricating prototype diodes this type of curve is seen quite often when the "blocking" contact fails or the diode is partially shorted by conductive surface states.

\* Physics of Semiconductor Devices, S. M. Sze.

† Figure number used in original Chinese text.

A second set of experiments was carried out with apparently the same type of photodiode:

- The output of the diode has been amplified by a "radiometer" amplifier. It is not clear whether the diode is reverse biased or used as a solar cell with only the carrier diffusion length as an active volume.
- With "normal" children the amplified output was  $10^{-5}$ - $10^{-6}$  W/cm<sup>2</sup>.
- With "exceptional" children bursts of signal (noise?) were observed up to  $10^{-2}$ - $10^{-3}$  W/cm<sup>2</sup> over periods of several minutes.

#### Analysis

The results of both sets of experiments are open to several explanations due to the ambiguous nature of the experimental procedure.

- The change in I/V characteristic could be due to simple heating of the diode. Attachments one and two both show how leakage current varies with temperature. A  $10^0$ C rise above ambient could be expected from a hand-held device, resulting in a larger leakage current. In addition, the breakdown knee will sometimes move toward lower voltages as the temperature rises resulting in noise or breakdown bursts. Finally, surface states which are not seen at room temperature may become active at higher temperatures resulting in the hysteresis seen in the "exceptional" I/V characteristics.
- If the diode and its container are not adequately electrically shielded, the effect of holding the assembly in one's hand would be to add components of stray resistance and capacitance to the output signal. This effect would be similar to that shown in Figure 2b. Anyone who has worked with electrometers is familiar with this effect. The usual cure is to use BNC connectors and coaxial cable.
- Finally, the infrared radiation associated with a black body at skin temperature (310K maximum) might cause some of the signals seen in the second set of experiments. In particular, a warmer than room temperature diode could

be operating in an already high leakage condition whereby extra input (static charge, IR radiation) might initiate carrier avalanche--yielding large noise bursts. Attached are several pages of figures and calculations which demonstrate that the sensitivity of the detector lies clearly in the IR region. Furthermore, application of the Stefan-Boltzmann law demonstrates that  $\sim 5 \times 10^{-3} \text{ W/cm}^2$  may be available from a black body of 10% efficiency. However the peak of the distribution falls at about  $9-10 \mu$ . At this wavelength neither a silicon or germanium diode is very efficient. This result suggests one of the two preceding mechanisms as a more likely candidate.

## Comments on "Abstract"

- Photodiode sensitivity extends into IR  
 $\text{VISIBLE} \approx 0.4\mu \text{ to } 0.7\mu \text{ @ } 1\% \text{ f max}$   
 $(\text{STANDARD OBSERVER}) \quad (0.550\mu)$
- IR  $\approx 0.7\mu \rightarrow 10^3\mu$
- Diode (from paper)  $\propto 0.190 \text{ to } 1.1\mu$   
- if Silicon max efficiency @  $0.73\mu$
- Black paper does not alter "effect" on diode.
- $R_c = \epsilon \sigma T^4$  (STEFAN-BOLTZMANN)  
where:  $R_c = \text{W/cm}^2$ ,  $\epsilon = \text{emissivity}$   
 $\sigma = 5.67 \times 10^{-8} \text{ W/m}^2 \text{ K}^4$   
if  $T = 37^\circ\text{C} + 273 = 310^\circ\text{K}$ 

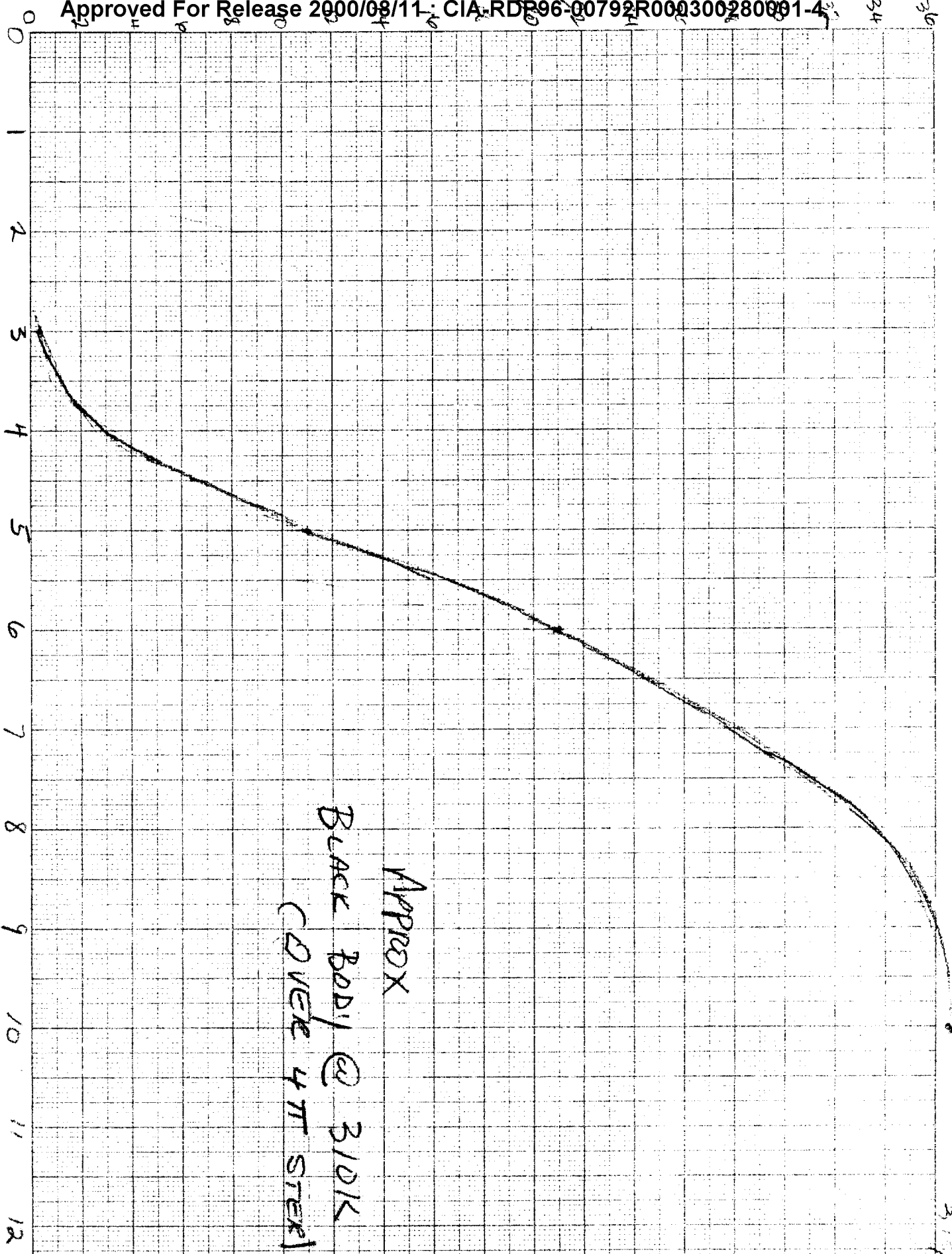
$$T^4 = 9.235 \times 10^9 \text{ (100cm)}^2$$

$$R_c = 5.24 \times 10^{-2} \text{ W/M}^2 \epsilon$$

$$= 5.24 \times 10^{-2} \text{ W/cm}^2 \epsilon \text{ overall } \Delta\lambda$$
- if  $\epsilon = 10^3$ 

$$R_c = \underline{5.24 \times 10^{-3} \text{ W/cm}^2 \text{ overall } \Delta\lambda}$$

$$= 3.63 \times 10^{-1} \text{ W/cm}^2 \text{ dA}$$



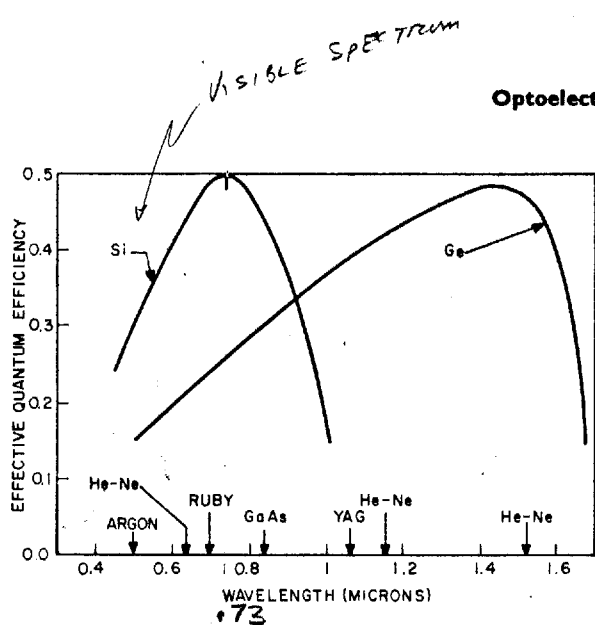


Fig. 24 Effective quantum efficiency (hole-electron pairs/photon) versus wavelength for Ge and Si photodetectors.  
(After Melchior and Lynch, Ref. 39.)

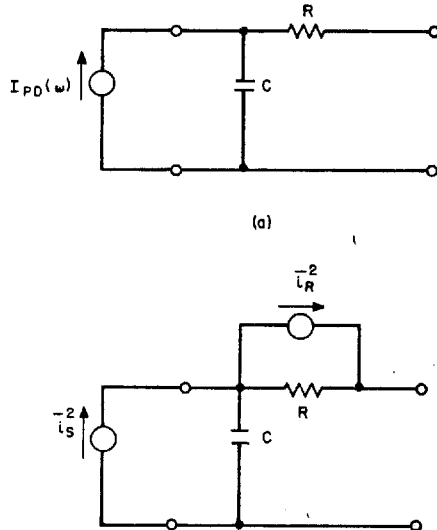


Fig. 25  
(a) Equivalent circuit and  
(b) noise equivalent circuit of a photodiode, where  $R$  is the series resistance and  $C$  is the junction capacitance.  
(After DiDomenico and Svelto, Ref. 35.)

#### 4 Photodetectors

available power for the photo

$$P_{av} = \frac{1}{8} |I_{PD}(\omega)|$$

It is interesting to compare  $E$  For a typical photodiode with a photoconductor with the same available power from the phot from the photoconductor.

The signal-to-noise perform equivalent noise circuit shown noise source due to the series source. The signal-to-noise ra

$$(S/N)_{\text{power}} = \frac{\eta}{4I}$$

Comparing Eq. (44) with Eq. at high-level detection where SNR is comparable; at low-lev however, the SNR of the pho

**B. The p-i-n Photodiode**  
depletion-layer photodiode. (the intrinsic layer) can be tai frequency response. A typical Fig. 26(a). Absorption of ligh pairs. Pairs produced in the de will eventually be separated by external circuit as carriers drift

Under steady-state conditio biased depletion layer is given

where  $J_{dr}$  is the drift current region and  $J_{diff}$  is the diffusior side the depletion layer in the reverse-biased junction. We s assumptions that the thermal g surface  $n$  layer is much thinner electron generation rate is give

## DETECTORS AND DETECTOR SYSTEMS

## SILICON CHARGED-PARTICLE DETECTORS

characteristics. The detector changes include increased noise and changes in voltage drop across the load resistor, which require adjustments to the applied bias voltage, which in turn change the electric-field strength. Thus carrier trapping and increased detector noise are degrading to energy resolution.

Resolution degradation appears as a broadening of the response for a monoenergetic source. With increasing doses of neutrons, charged particles, or fission fragments, the low-energy side of the response peak may begin to show a definite secondary peak. Continued irradiation results in further broadening, until, in extreme cases, the multiple peaks may merge completely. Electron bombardment tends to increase leakage current, resulting in excess detector noise, which broadens response peaks. Some of these damage effects may undergo a degree of annealing, but there is always a significant residual deterioration after a sufficient dose has been accumulated.

Partially depleted detectors are more susceptible than are fully depleted devices to deterioration from radiation damage. Radiation damage for different types of detectors are compared in Table 2, which gives the dose for various particles to significantly deteriorate the detectors.

## OPERATING TEMPERATURE

As a rule of thumb, increasing the operating temperature of a charged-particle detector causes the leakage current to increase by a factor of 3 for each  $10^{\circ}\text{C}$  rise, resulting in a noise-width increase of approximately 1.7 keV per  $10^{\circ}\text{C}$  rise. The upper temperature limit is determined by the maximum acceptable noise or by the ultimate breakdown of the detector (usually between 45 and  $55^{\circ}\text{C}$ ). The effects of high-temperature breakdown are permanent and are not covered by the warranty terms. An additional effect is the shift in detector bias caused by the higher leakage current. This leak-

age current increases the voltage drop across the series bias resistor, thus lowering the bias voltage across the detector. When high-temperature operation is necessary, a constant sensitive depth is maintained over the entire operating temperature range only if a totally depleted detector is used with sufficient overbias to compensate for the drop across the series bias resistor, which should be as small as possible (usually 1 to  $3\text{ M}\Omega$  is adequate).

Decreasing the operating temperature of the detector reduces junction noise and leakage current. However, the capacitance of the device is a constant limiting parameter of the system noise. Another limitation to successful operation at low temperatures is the expansion coefficient of the detector's component parts. The expansion coefficient is similar for silicon and for lavite, the ring in which the silicon wafer is mounted, but is quite different for the bonding epoxy. Therefore at very low temperatures the epoxy may crack, causing excessive noise or loss of contact. The probability of low-temperature damage increases with detector size. For cooled operation, detectors fabricated with cryogenic epoxy may be special ordered from ORTEC.

Another effect of decreasing the operating temperature of a silicon detector is an increase of the average energy necessary to create an electron-hole pair,  $\epsilon$ . Due to a widening of the bandgap of silicon in the temperature range from 300 K to 80 K,  $\epsilon$  increases from 3.62 eV to 3.72 eV. A result of this increase is an apparent shift in energy of a measured spectroscopic line. For instance, Fig. 8 shows the apparent peak shift of the 5.477-MeV  $^{241}\text{Am}$  alpha particle peak in the 4.2-K to 320-K temperature range measured with silicon charged-particle detectors.

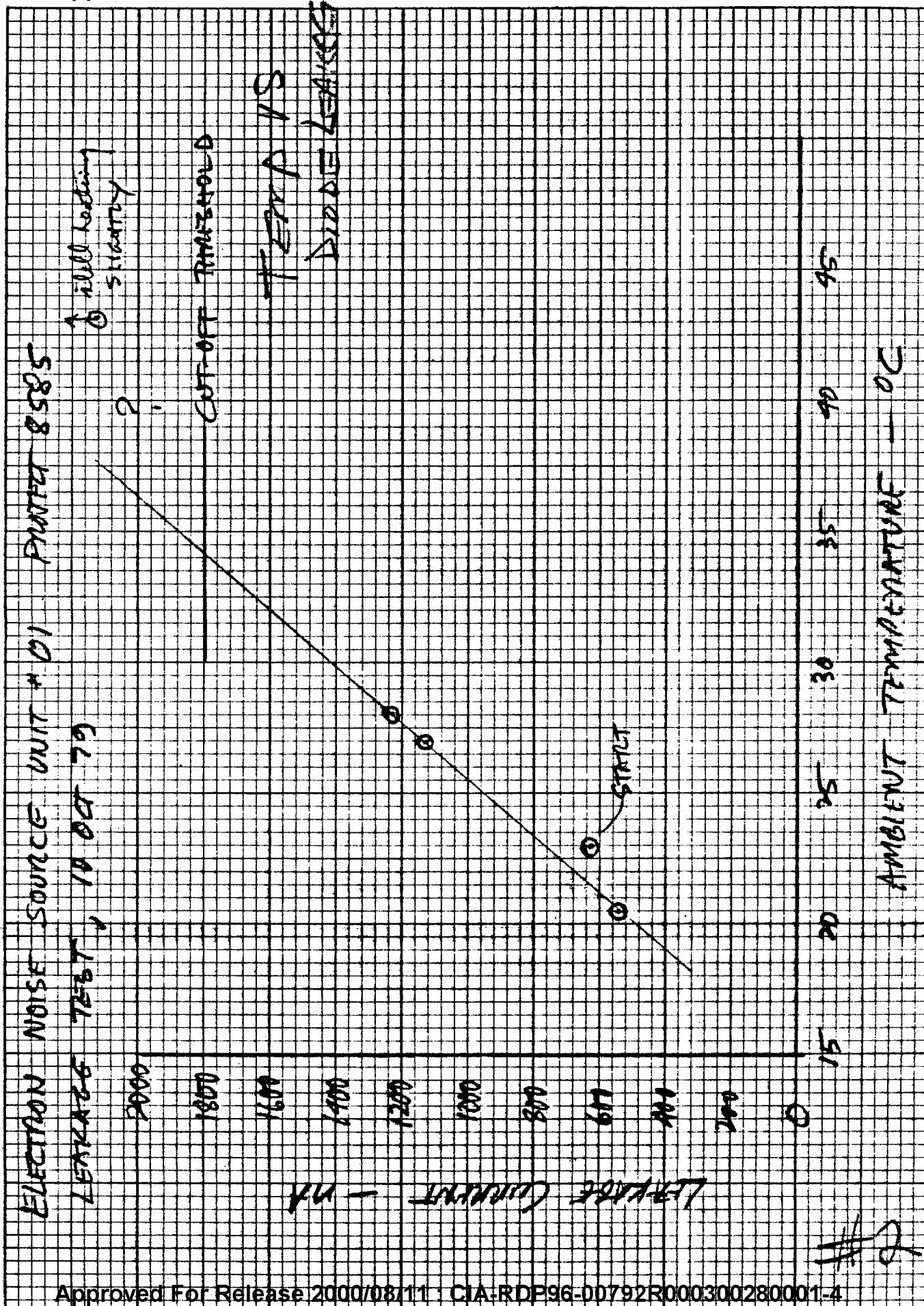
## SHOCK AND VIBRATION

Many ORTEC surface-barrier detectors have been subjected to the shock and vibration tests required for

Table 2. Comparison of Radiation Damage in Silicon and Germanium Particle Detectors

Type of Detector	Radiation Damage (particles/cm <sup>2</sup> )				
	Electrons	Fast Neutrons	Protons	Alpha Particles	Fission Fragments
Surface barrier	$10^{13}$	$10^{12}$	$10^{10}$	$10^9$	$10^8$
Diffusion junction	$10^{13}$	$10^{12}$	$10^{10}$	$10^9$	$10^8$
Si(Li)	$10^{12}$	$10^{11}$	$10^8$ - $10^9$		
Ge(Li)			$10^8$ - $10^9$		

# /



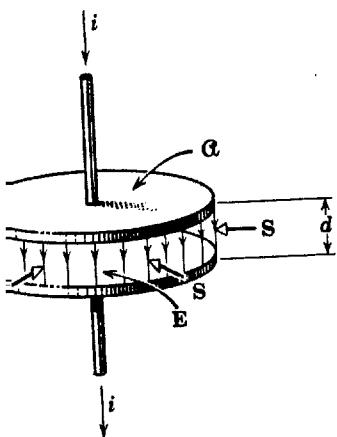


Fig. 39-17

ing charged. (a) Show that the total volume. (b) Show that calculated by integrating the Poynting is equal to the rate at which the

energy density for all points within the Poynting vector point of view, through the wires but through the space we must first find  $\mathbf{B}$ , which is the ring the charging process; see Fig.

## Nature and Propagation of Light

### CHAPTER 40

#### 40-1 Light and the Electromagnetic Spectrum

Light was shown by Maxwell to be a component of the *electromagnetic spectrum* of Fig. 40-1. All these waves are electromagnetic in nature and have the same speed  $c$  in free space. They differ in wavelength (and thus in frequency) only, which means that the sources that give rise to them and the instruments used to make measurements with them are rather different.\* The electromagnetic spectrum has no definite upper or lower limit. The labeled regions in Fig. 40-1 represent frequency intervals within which a common body of experimental technique, such as common sources and common detectors, exists. All such regions overlap. For example, we can produce radiation of wavelength  $10^{-3}$  meter either by microwave techniques (microwave oscillators) or by infrared techniques (incandescent sources).

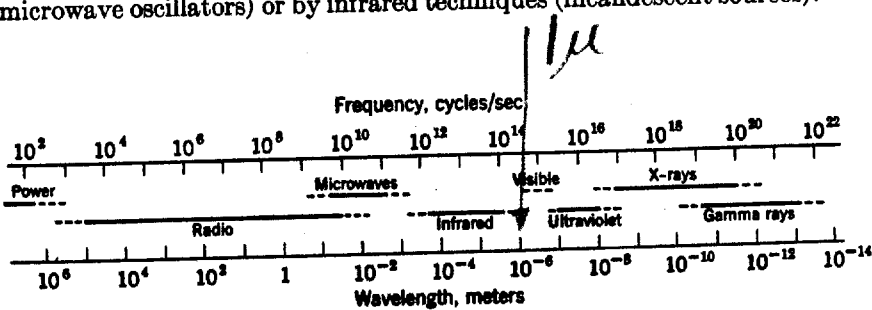


Fig. 40-1 The electromagnetic spectrum. Note that the wavelength and frequency scales are logarithmic.

\* For a report of electromagnetic waves with wavelengths as long as  $1.9 \times 10^7$  miles the student should consult an article by James Heitzler in the *Scientific American* for March 1962.

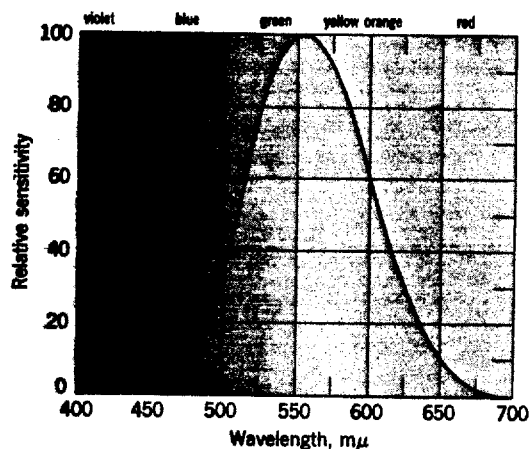


Fig. 40-2 The relative eye sensitivity of an assumed *standard observer* at different wavelengths for normal levels of illumination. The shaded areas represent the (continuously graded) color sensations for normal vision.

"Light" is defined here as radiation that can affect the eye. Figure 40-2, which shows the relative eye sensitivity of an assumed *standard observer* to radiations of various wavelengths, shows that the center of the visible region is about  $5.55 \times 10^{-7}$  meter. Light of this wavelength produces the sensation of yellow-green.\*

In optics we often use the micron (abbr.  $\mu$ ) the millimicron (abbr.  $m\mu$ ), and the Angstrom (abbr. A) as units of wavelength. They are defined from

$$1 \mu = 10^{-6} \text{ meter}$$

$$1 m\mu = 10^{-9} \text{ meter}$$

$$1 \text{ A} = 10^{-10} \text{ meter.}$$

Thus the center of the visible region can be expressed as  $0.555 \mu$ ,  $555 m\mu$ , or  $5550 \text{ A}$ .

The limits of the visible spectrum are not well defined because the eye sensitivity curve approaches the axis asymptotically at both long and short wavelengths. If the limits are taken, arbitrarily, as the wavelengths at which the eye sensitivity has dropped to 1% of its maximum value, these limits are about 4300 A and 6900 A, less than a factor of two in wavelength. The eye can detect radiation beyond these limits if it is intense enough. In many experiments in physics one can use photographic plates or light-sensitive electronic detectors in place of the human eye.

\* See "Experiments in Color Vision" by Edwin H. Land, *Scientific American*, May 1959, and especially "Color and Perception: the Work of Edwin Land in the Light of Current Concepts" by M. H. Wilson and R. W. Brocklebank, *Contemporary Physics*, December 1961, for a fascinating discussion of the problems of perception and the distinction between color as a characteristic of light and color as a perceived property of objects.